2012 NDIA GROUND VEHICLE SYSTEMS ENGINEERING AND TECHNOLOGY SYMPOSIUM
VEHICLE ELECTRONICS AND ARCHITECTURE (VEA) MINI-SYMPOSIUM
AUGUST 14-16, MICHIGAN

RESEARCH OF THE EFFECTS OF INTEGRATION INTO ARMOR ON THE PERFORMANCE OF SPINTRONIC MICROWAVE DETECTORS

Elena Bankowski, PhD
E-mail: elena.n.bankowski.civ@mail.mil
Thomas Meitzler, PhD
Tomas Pesys
TARDEC
Warren, MI

ABSTRACT

The authors studied the effects of different types of armor on the performance of spin-torque microwave detectors (STMD). Working prototypes of novel nano-sized spintronic sensors of microwave radiation for battlefield anti-radar and wireless communications applications are being integrated into Sensor Enhanced Armor (SEA) and Multifunctional Armor (MFA) and tested in SEA-NDE Lab at TARDEC. The preliminary theoretical estimations have shown that STMD based on the spin-torque effect in magnetic tunnel junctions (MTJ), when placed in the external electromagnetic field of a microwave frequency, can work as diode detectors with the maximum theoretical sensitivity of 1000 V/W. These STNO detectors could be scaled to sub-micron size, are frequency-selective and tunable, and are tolerant to ionizing radiation. We studied the performance of a STMD in two different dynamical regimes of detector operation: in well-known traditional in-plane regime of STMD operation and in recently discovered novel out-of-plane regime.

INTRODUCTION

The spin-transfer-torque (STT) effect in magnetic multilayers theoretically predicted in [1, 2] and experimentally observed in [3–13] provides a new method of manipulation of magnetization direction in nano-magnetic systems [14]: magnetization switching [3, 4], generation of microwave oscillations under the action of DC electric current [5–11] and the spin torque diode effect [12–13], which can be used for the development of practical microwave detectors, so called spin-torque microwave detectors (STMD), and also for quantitatively measuring STT [15, 16].

The spin torque diode effect is a quadratic rectification effect of the input microwave current $I_{RF}(t)$ in a magnetoresistive junction, which is commonly observed in traditional regime of operation of a STMD, when the frequency f of the current $I_{RF}(t) = I_{RF}\sin(2\pi ft)$ is close to the ferromagnetic resonance (FMR) frequency f_0 of the junction. In this case the resonance oscillations of the junction resistance $R(t)$ (at frequency f_0) can ineract with the oscillations of input microwave current $I_{RF}(t)$ (at frequency $f \approx f_0$) and produce a relatively large output DC voltage $U_{DC} = \langle I_{RF}(t)R(t)\rangle$ across the junction (here $\langle ...\rangle$ denotes averaging over the period of oscillations $1/f$).

In the traditional regime of operation of a STMD [12, 13, 17] STT excites a *small-angle in-plane* (IP) magnetization precession about the equilibrium direction of magnetization in the FL of a magnetic tunnel junction (MTJ) (see the red

dashed curve in Figure 1). Below we refer to this regime of STMD operation as the IP-regime.

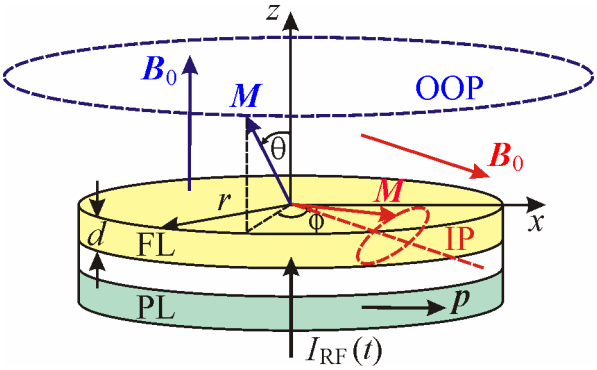

Figure 1. The model of a STMD: circular nano-pillar of radius r consists of the "free" magnetic layer (FL) of thickness d and the "pinned" magnetic layer (PL). Under the action of microwave current $I_{RF}(t)$ magnetization vector **M** (shown by a blue or red arrow) is precessing along small-angle in-plane (red dashed curve, IP-regime) or large-angle out-of-plane (blue dashed curve, OOP-regime) trajectory about the direction of the bias magnetic field $\mathbf{B}_0$ (shown by a red or blue arrow), **p** = **x** is the unit vector in the direction of the magnetization of the PL, **x** is the unit vectors of x-axis.

Using analytical theory we have shown that the performance of a passive STMD in IP-regime was limited by a thermal noise. We have also shown how to calculate the optimal parameters of a STMD operating in this regime. We used the developed formalism for optimization of practical noise-handling properties of a STMD.

In comparison to the well-known IP-regime of STMD operation, we also considered a different regime of operation of an STMD, based on the excitation of *large-angle out-of-plane* (OOP) magnetization precession under the influence of the input microwave current $I_{RF}(t)$ (see the blue dashed curve in Figure 1). Using analytical and numerical calculations, we have shown that all the major STMD characteristics in the OOP-regime qualitatively differ from the ones in the traditional IP-regime. In particular, excitations in the OOP-regime do not have a resonance character and exist in a wide range of driving frequencies. Also, the output DC voltage of an STMD in the OOP regime is almost independent of the input microwave power, provided it exceeds a certain threshold value. We believe that these properties of an STMD in the OOP-regime will be useful for the development of nano-sized threshold detectors with a large output DC voltage and also for the applications in microwave energy harvesting in the low-frequency region of the microwave band.

PROPERTIES OF A RESONANCE-TYPE STMD

It has been shown in [16, 17] that a magnetic tunnel junction (MTJ) subject to the external microwave current $I_{RF}(t) = I_{RF}cos(2\pi ft)$ can perform as a resonance-type quadratic detector of microwave radiation generating the DC voltage U_{DC} proportional to the acting microwave power $U_{DC} = \varepsilon P_{RF}$ ($P_{RF} \sim I_{RF}^2$). The detector operation is based on the spin-torque effect [1, 2] and the detector sensitivity ε has the maximum value $\varepsilon = \varepsilon_{res}$ when the frequency of the external microwave signal is close to the eigen-frequency f_0 of the MTJ nanopillar, $f = f_0$. The resonance sensitivity ε_{res} of the STMD was calculated in [18]:

$$\varepsilon_{res} = \frac{U_{DC}}{P_{RF}} = \left(\frac{\gamma h}{8\pi e}\right)\frac{P^3}{M_s V \Gamma} Q(\theta_0), \qquad (1)$$

where $\gamma \approx 2\pi \cdot 28$ GHz/T is the modulus of the Gyromagnetic ratio, h is the Planck constant, e is the modulus of the electron charge, P is the spin-polarization efficiency of the MTJ, Ms is the saturation magnetization of the free layer (FL) of MTJ, $V = \pi r^2 d$ is the volume of the FL (r is its radius and d is its thickness), Γ is the magnetization damping rate in the MTJ FL, proportional to the Gilbert damping constant α, and $Q(\theta_0)$ is the geometrical factor that depends on the angle θ_0 between the directions of the

equilibrium magnetization in FL and pinned layer (PL) of the MTJ.

We are introducing the microwave powers $P_{RF}= U_{DC}/\varepsilon_{res}$, the noise power $P_{JN} = U_{JN} / \varepsilon_{res}$ and U_{JN} - the voltage associated with Johnson-Nyquist (JN) noise. Also, using the noise power $P_{MN} = \frac{P_{MN}}{\varepsilon_{res}}$ and U_{MN} as the voltage associated with the magnetic (MN) noise in the FL of the MTJ, we can write a simple expression for the signal-to-noise ratio (SNR) of the STMD in terms of these characteristic powers. The SNR of a STMD can be calculated as:

$$SNR = \frac{U_{DC}}{\Delta U_{DC}} = \frac{P_{RF}}{P_{JN}} \sqrt{\frac{P_{MN}}{P_{MN} + P_{RF}}}, \qquad (2)$$

The simple analysis of Equation (2) demonstrates that there are two distinct regimes of operation of the resonance STMD in the presence of thermal noise. We shall classify them by the type of noise that limits the minimum detectable power of STMD *P*min (power corresponding to SNR = 1).

The first regime corresponds to the case of relatively high frequencies of the input microwave signal, when $P_{MN} \gg P_{RF}$ (for $P_{RF} \sim P$min). In this regime, similar to the conventional semiconductor diodes, the minimum detectable power is limited by the low-frequency JN noise, Pmin = P_{JN}, and the SNR of STMD is linearly proportional to the input microwave power P_{RF} (SNR ≅ P_{RF}/P_{JN}).

The second regime takes place in the opposite limiting case of relatively low input frequencies, when $P_{MN} \ll P_{RF}$. In this case the SNR of STMD increases with *P*RF much slower than in conventional diodes, and is proportional to the square root of the input microwave power: SNR≅ $\sqrt{P_{RF}/P_{JN}}$. The minimum detectable power *P*min= P_{JN}^2/P_{MN} in this regime is limited by the magnetic noise in the FL of the MTJ.

The existence of two distinct regimes of STMD operation is illustrated in Figure 2 below, where two curves calculated from Equation (2) show the STMD SNR as functions of the input power for signal frequencies f_1 = 1 GHz (dashed blue line) and f_2 = 25 GHz (red solid curve).

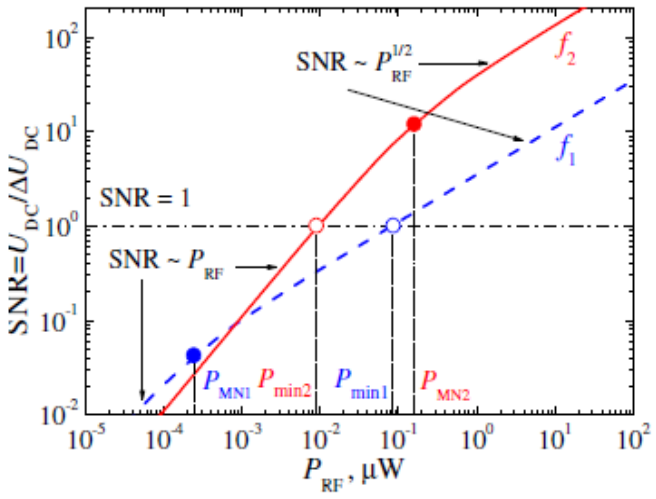

Figure 2. Dependence of the SNR of STMD on the input microwave power P_{RF} calculated from Eq. (2) for two different frequencies of the input microwave signal: f_1 = 1 GHz (dashed blue line) and f_2 = 25 GHz (solid red line). P_{min} is the minimum detectable power of the STMD (at SNR = 1).

EXPERIMENTAL SETUP

The authors have measured the microwave signals transmitted through ceramic and composite materials and detected by the STMD. The output signal was rectified by the STMD detector and was measured using a nanovoltmeter. The experiment was setup inside a grounded anechoic chamber so that ambient signals did not interfere with testing. Microwave signals were transmitted by a horn antenna and received by the STMD detector, shown in Figure 3. Various armor samples were positioned in front of the STMD detector (aluminum oxide shown).

The data were collected using both the traditional in-plane (IP) regime of the STMD operation and the recently discovered novel out-of-plane (OOP)

regime of the STMD operation. Detectors labeled as 1A, 2A, 3A, 4A and 5A were IP detectors. Detectors labeled as 1B, 2B, 3B, 4B and 5B were OOP detectors. The antennae feature a set screw that was used to adjust the position of the external magnet, determining the magnitude of the external magnetic field the sensor was subjected to. The enlarged view of the STMD detector is shown in Figure 4 [19].

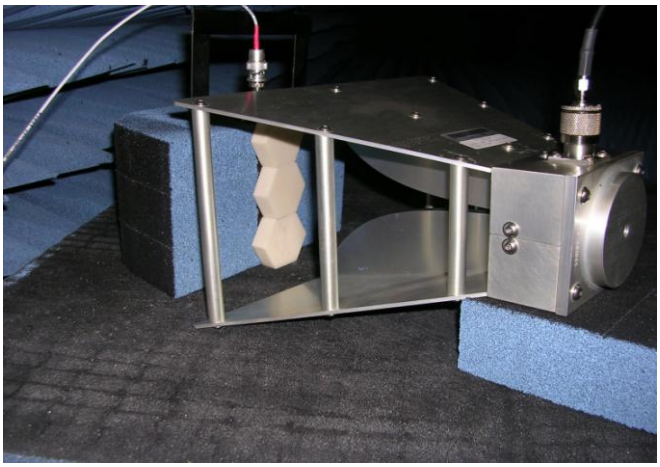

Figure 3. The experimental setup inside the anechoic chamber for measuring microwave signals using the transmitting horn antenna and the STMD detector. The aluminum oxide armor cells were positioned in front of the detector.

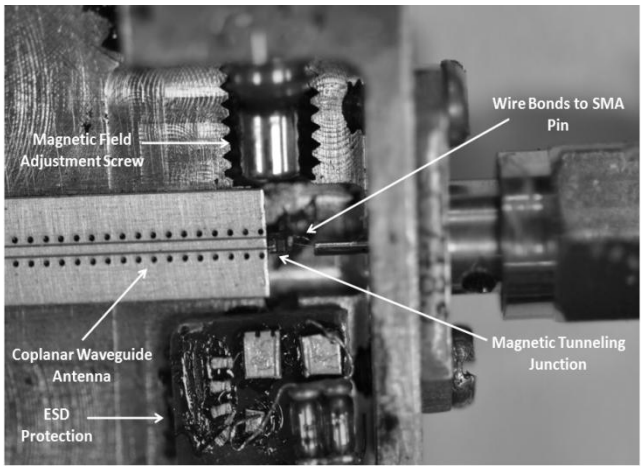

Figure 5. Enlarged view of the STMD [19].

The external magnetic field was adjusted in our experiments in order to achieve the maximum sensitivity of the STMD detector. The data that were collected using the traditional in-plane (IP) regime of STMD operation (sensor # 4A) are shown in Figure 5 below. The data collected using the novel out-of-plane (OOP) regime of STMD operation (sensor # 3B) are shown in Figure 6. These plots were compared with the baseline data collected with and without ceramics cells using the experimental setup shown in Figure 3. The comparison shows that there was no attenuation of the incoming RF signal going through ceramics cells: Aluminum oxide and SiC, see Figure 5 and 6. In some cases we observed the increase in the output voltage, when the microwave signal was going through a ceramic material.

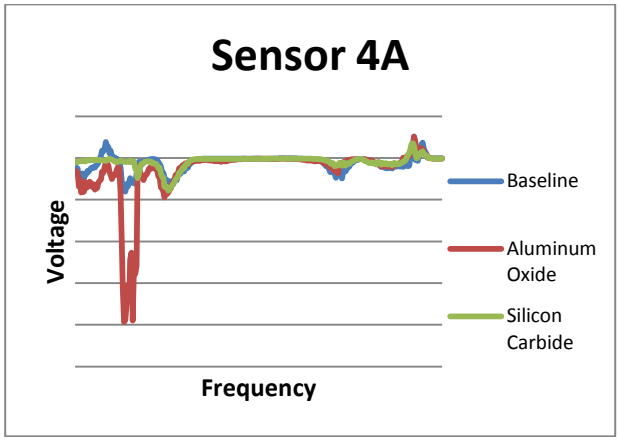

Figure 5. The output spintronic detector data were collected using the traditional in-plane (IP) regime of STMD operation inside the anechoic chamber.

This effect may be due to a microwave resonator being formed, i.e. cavity resonance of the brass cover of the STMD detector and the intervening ceramic material.

As shown by the data and graphs, in general there was little to no voltage drop compared to the baseline performance, specified as nothing between the transmitting antenna and STMD

detector. At other frequencies, the performance did suffer due to an intervening material compared to the baseline.

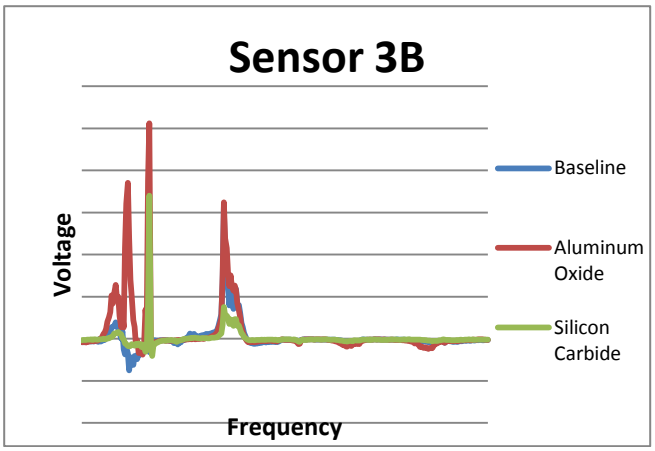

Figure 6. The output spintronic detector data were collected using the novel out-of-plane (OOP) regime of STMD operation (detector # 3B) inside the anechoic chamber.

CONCLUSION

Further experimentation and numerical simulation is planned to validate and explain these results. Measurements are performed while the STMD is enclosed in a grounded anechoic chamber so that background emissions have a negligible effect on the amplitude and frequency of the resonance peaks. The cavity resonance effect of an enclosed and embedded STMD, when further validated and modeled, may have important applications in spectrum analysis of incoming signals, RF energy harvesting and multifunctional armor.

REFERENCES

[1] J.C. Slonczewski, J. Mag. Mag. Mat. **159**, L1 (1996); J. Mag. Mag. Mat. **195**, L261 (1999).
[2] L. Berger, Phys. Rev. B **54**, 9353 (1996).
[3] J.A. Katine, F.J. Albert, R.A. Buhrman, E.B. Myers, and D.C. Ralph, Phys. Rev. Lett. **84**, 3149 (2000).
[4] S. Urazhdin, N. O. Birge, W. P. Pratt, Jr., and J. Bass, Phys. Rev. Lett. **91**, 146803 (2003).
[5] S.I. Kiselev, J.C. Sankey, I.N. Krivorotov, N.C. Emley, R.J. Schoelkopf, R.A. Buhrman, and D.C. Ralph, Nature (London) **425**, 308 (2003).
[6] S. Kaka, M.R. Pufall, W. H. Rippard, T. J. Silva, S.E. Russek, and J.A. Katine, Nature (London) **437**, 389 (2005).
[7] K. J. Lee, A. Deac, O. Redon, J.-P. Nozières, and B. Dieny, Nature Mater. **3**, 877 (2004).
[8] I.N. Krivorotov, N.C. Emley, J.C. Sankey, S.I. Kiselev, D.C. Ralph, and R.A. Buhrman, Science **307**, 228 (2005).
[9] F.B. Mancoff, N.D. Rizzo, B.N. Engel and S. Tehrani, Nature **437**, 393 (2005).
[10] D. Houssameddine, U. Ebels, B. Delaët, B. Rodmacq, I. Firastrau, F. Ponthenier, M. Brunet, C. Thirion, J.-P. Michel, L. Prejbeanu-Buda, M.-C. Cyrille, O. Redon, and B. Dieny, Nature Mater. **6**, 447 (2007).
[11] Ruotolo, V. Cros, B. Georges, A. Dussaux, J. Grollier, C. Deranlot, R. Slavin, and V. Tiberkevich, IEEE Trans. Magn. **45**, 1875 (2009).
[12] J.C. Sankey, Y. Cui, J.Z. Sun, J.C. Slonczewski, R.A. Buhrman, and D.C. Ralph, Nat. Phys. **4**, 67 (2008).
[13] C. Wang, Y.-T. Cui, J.Z. Sun, J.A. Katine, R.A. Buhrman, and D.C. Ralph, Phys. Rev. B **79**, 224416 (2009).
[14] C. Wang, Y.-T. Cui, J.Z. Sun, J.A. Katine, R.A. Buhrman, and D.C. Ralph, J. Appl. Phys. **106**, 053905 (2009).
[15] Guillemet, K. Bouzehouane, S. Fusil and A. Fert, Nature Nanotech. **4**, 528 (2009).
[16] A.A. Tulapurkar, Y. Suzuki, A. Fukushima, et al., Nature **438**, 339 (2005).
[17] S. Ishibashi, T. Seki, T. Nozaki, H. Kubota, et al., Appl. Phys. Express **3**, 073001 (2010).
[18] C. Wang, Y.-T. Cui, J. Z. Sun *et al.*, J. Appl. Phys. **106**, 053905 (2009).
[19] E. Bankowski, T. Meitzler, S. Zielinski et al., Antenna development for multi-functional armor, Proceedings of GVSETS, August 2011, Dearborn, MI.